PROCEEDINGS of the
23rd International Congress on Acoustics

9 to 13 September 2019 in Aachen, Germany

A Computational Investigation into the Influence of the Shear Properties of the Seabed on Sound Propagation in Shallow Water.

Ray KIRBY[1]; Wenbo DUAN[2];

[1] University of Technology, Sydney, Australia

[2] Brunel University London, United Kingdom

ABSTRACT

The propagation of sound waves in the ocean is influenced by the acoustic characteristics of the seabed, especially in shallow water. If the seabed is considered to be an elastic or viscoelastic structure, then sound propagation will be influenced by the shear and longitudinal properties of this structure. Accordingly, this paper examines the sensitivity of sound propagation to the shear properties of the ocean floor for shallow waters and when the sound source lies in the ocean. This is motivated by predictions reported in the structural mechanics literature, which demonstrate that wave propagation in viscoelastic structures can be highly sensitive to the shear properties of the material. This investigation uses the semi analytic finite element method to undertake a set of numerical experiments. This numerical approach provides a computationally efficient way of solving the fully coupled acoustic problem, with Bergmann's equation used for the fluid, and Navier's elastodynamic wave equation for the seabed. Both elastic and viscoelastic structures are examined and predictions are reported for a range of shear properties, and the relative sensitivity of sound propagation on these shear properties is then investigated.

Keywords: Sound propagation, Shallow ocean, Shear waves

1. INTRODUCTION

The propagation of sound in the ocean depends on the acoustic properties of the seabed, as well as those of the ocean. This forms a coupled system so that sound propagation from a point source located in the sea depends on the viscoelastic properties of the seabed. Accordingly, to compute accurately sound propagation in an ocean waveguide it is necessary to capture the physics of the propagating viscoelastic wave. This demands the use of the elastodynamic wave equation and the inclusion of both compressional and shear waves. This delivers a complex coupled system and developing accurate theoretical models is challenging, and this is especially true for shallow oceans where the coupling effects are likely to be strong and complex interactions between the ocean and a layered seabed must be accounted for.

The development of computational models for ocean acoustics has largely focused on advancing the pioneering work of Pekeris (1). This involves separating variables in order to recast the problem into two separate wave equations in the range (r) and depth (z) directions. To solve the depth dependent wave equation, a modal expansion is often applied so that the pressure and displacement are written as a sum over downwards and upwards propagating planar waves (2, 3). This enables reflections from the interface between the ocean and the seabed to be captured, as well as those reflections from layers inside the seabed. The range dependence is then captured using Hankel functions, or large argument approximations of Hankel functions, so that sound propagation from a sound source located in the ocean can be computed. This approach has led to the development of a large number of computational codes (4), the majority of which adopt varying approaches to solve the depth dependent eigenproblem. Popular examples include the analytic approach of Westwood et al. (5) and the numerical solutions to the depth dependent wave equation by Porter and Reiss (6, 7). These

[1] ray.kirby@uts.edu.au
[2] wenbo.duan@brunel.ac.uk

methods are widely used to compute the sound pressure field inside the ocean, and they are suitable for including the viscoelastic behavior of the seabed. However, it is challenging to capture the entire physics of the problem using these methods, especially for shallow waters. This is because of the strong coupling present in shallow waters, where it is common for large numbers of eigenmodes to be required in order to obtain accurate predictions. Ensuring all relevant modes have been captured, as well as accommodating the complex scattering inside the seabed is challenging. Furthermore, enforcing the correct limiting boundary conditions in the seabed is also important for shallow water predictions and this is also difficult to capture accurately when using a Pekeris style approach.

This article uses a different approach that is based on the semi analytic finite element (SAFE) method (8-11). This approach discretizes the depth and then solves an eigenproblem for the range direction, so that the modes obtained are forward and backwards propagating modes. This approach enables the inclusion of depth dependent acoustic properties in the ocean, as well as the correct coupling conditions between each layer in the waveguide. The application of a perfectly matched layer (PML) also enables the correct limiting boundary conditions to be applied in the depth direction. This method is then used here to explore sound propagation in relatively shallow oceans and the influence of shear waves is examined through the modification of the acoustic properties of the seabed. This study is undertaken in order to gain a better understanding of the importance of shear waves on the calculation of sound propagation in shallow oceans.

2. THEORY

The geometry of the ocean waveguide us shown in Fig. 1.

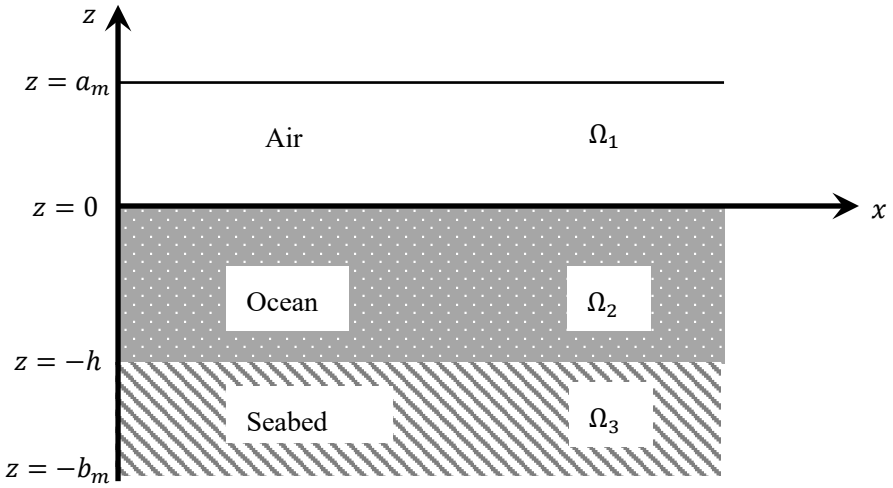

Figure 1 – Geometry of ocean waveguide.

The waveguide consists of three regions, Ω_1 which contains air above the ocean, Ω_2 is the ocean in which depth dependent properties can be included, and Ω_3 is a viscoelastic seabed. The wave equation for sound propagation in a fluid (Ω_1 or Ω_2) is given as (12)

$$\rho_{1,2}(z)\nabla\cdot\left(\frac{1}{\rho_{1,2}(z)}\nabla p'_{1,2}\right)-\frac{1}{c^2_{1,2}(z)}\frac{\partial^2 p'_{1,2}}{\partial t^2}=0 \tag{1}$$

where, p' is acoustic pressure, t is time, c is the speed of sound and ρ is the fluid density (these are assumed to be depth dependent only in Ω_2). The seabed is considered to be an elastic solid that supports both shear and compressional waves, and here the elastodynamic wave equation gives (13)

$$\nabla\cdot\boldsymbol{\sigma}'_3-\rho_3\frac{\partial^2\mathbf{u}'_3}{\partial t^2}=0 \tag{2}$$

where $\boldsymbol{\sigma}'_3$ is the Cauchy stress tensor, ρ_3 is the material density, and $\mathbf{u}'_3=[u'_{3x}\quad u'_{3z}]$ is the displacement in region Ω_3. These equation are solved by expanding the sound pressure field in each fluid, and the displacement in the seabed, over a set of eigenmodes propagating in the range direction, so that

$$p'_{1,2}(x,z,t) = \sum_{n=1}^{\infty} \mathrm{A}_n p^n_{1,2}(z) e^{i\omega t - ik_0\gamma_n x}, \tag{3}$$

$$\mathbf{u}'_3(x,z,t) = \sum_{n=1}^{\infty} \mathrm{A}_n \mathbf{u}^n_3(z) e^{i\omega t - ik_0\gamma_n x}, \tag{4}$$

where, $p^n_{1,2}(z)$, and $\mathbf{u}^n_3(z) = [u^n_{3x}(z) \quad u^n_{3z}(z)]$ are the eigenfunctions, and γ_n the eigenvalues. In addition, A_n are the modal amplitudes, k_0 is a reference wavenumber chosen so that γ is non-dimensional, where $k_0 = \omega/c_0$, ω is the radian frequency, c_0 is an (arbitrary) reference sound speed, and $i = \sqrt{-1}$.

To couple each wave equation together, it is necessary to apply the relevant boundary conditions. These are: continuity of pressure and particle velocity between each fluid region; continuity of pressure and normal stress, and continuity of normal displacement, between the fluid and the seabed; in addition, non-reflecting boundary conditions for $z \to \pm\infty$ are implemented using a PML. To apply these boundary conditions, the ansatz for each variable is substituted back into each wave equation and these are then weighted and integrated over the depth z. A SAFE formulation (8-11) is then applied that discretizes the depth dimension only, and in this article three noded quadratic line elements are used. The addition of the boundary conditions into the SAFE formulation then allows an eigenproblem to be solved for γ and the respective eigenfunctions.

Following solution of the eigenproblem, the sound propagation from a point source is calculated. This is realized using the method of Astley and Cummings (14), with the addition of the bi-orthogonality relation of Scandrett and Frenzen (15) to accommodate the viscoelastic seabed. This gives the modal amplitudes of the point source as:

$$\mathrm{A}_j = \frac{2}{k_0\gamma_j\Lambda_{j,j}} \frac{\rho_1}{\rho_s\rho_2(-h)c_0^2} p_{2,j}(z_s), \tag{4}$$

where, $\Lambda_{j,j}$ is an orthogonality relation (15), and ρ_s and z_s are the density and depth of the point source, respectively. Note that these modal amplitudes have been normalized against a reference point source, whose amplitude is equal to unity at a distance of 1 m. This then enables the sound transmission loss (TL) to be computed for the waveguide using a normalized TL common in the literature, so that

$$\mathrm{TL} = -20\log_{10}|p(x,z)|. \tag{5}$$

This expression for TL is then used in the calculations that follow in the next section. Note that these calculations are for a spherical point source and include cylindrical spreading.

3. RESULTS AND DISCUSSION

In this section a number of numerical experiments are carried out using the SAFE model described in the previous section. The SAFE model is a general approach that is well suited to analyzing shallow oceans, and so the focus in this section is on computing sound propagation in oceans of a depth of 100 m or less. Accordingly, the first set of numerical experiments uses an ocean of depth 100 m, with a source placed at a depth of 25 m, and a receiver at a depth of 75 m. The air above the ocean has a height of 20 m, and a PML of thickness 10 m. The seabed has an overall depth of 310 m, with a PML of depth 200 m. The finite element mesh uses 440 elements to solve the eigenproblem, and 400 modes to obtain the TL; this takes about 6 seconds to solve on a standard laptop.

The numerical tests use either sand or limestone in the seabed and their acoustic properties are listed in Table 1. In addition, the density of air and water are listed, where for simplicity the density and speed of sound in the ocean are assumed to be constant. In Fig. 2 the TL is calculated for a limestone seabed with zero damping; the shear velocity in the seabed is then varied in order to explore the influence of the shear properties of the seabed on the sound pressure field. It can be seen in Fig. 2 that significant changes in behavior are evident when the shear properties in the limestone are altered. For example, differences of up to 25 dB are seen for relatively modest changes in the shear velocity. It is however noticeable that for relatively short distances away from the sound source the differences

in TL are less pronounced, so that the effects of the shear properties on sound propagation in this waveguide are more evident for larger ranges.

Table 1 – Properties of waveguide

	Compressional Properties			Shear Properties	
	ρ (kg/m^3)	c_L (m/s)	α_L (dB/λ)	c_T (m/s)	α_T (dB/λ)
Sand	1400	1650	0.1	400	0.2
Limestone	2300	2500	0.05	1315	0.1
Water	1000	1500			
Air	1.2	343			

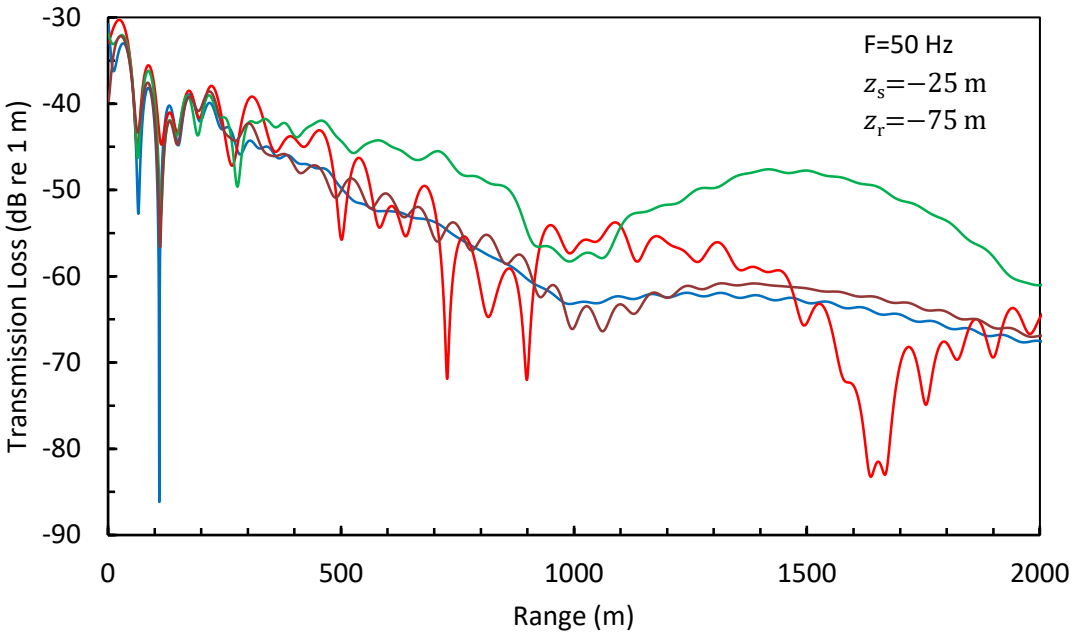

Figure 2 – TL for limestone seabed with zero damping. ——; $c_T = 1315$ m/s; ——; $c_T = 1000$ m/s; ——; $c_T = 1600$ m/s; ——; $c_T = 1200$ m/s.

In Fig. 3, damping is added into back into the limestone, with reference values taken from Table 1 ($\alpha_T = 0.1$ dB/λ). It is seen in Fig. 3 that the addition of damping has little effect on the TL, and that it is only in the longer ranges that a difference in behavior is noticeable. This lack of influence for the damping in the limestone is likely to be partly caused by the low excitation frequency, however these results do indicate that at least for this waveguide it is not so important to identify accurately the shear damping coefficient in the seabed.

In Fig. 4 predictions are shown for a more realistic waveguide in which a layer of sand 10 m deep is placed above a much thicker layer of limestone 300 m deep (including the PML). Figure 4 then investigates the influence of the shear properties of the sand (with damping) whilst keeping the properties of the limestone fixed (with damping). It is evident in Fig. 4 that significant differences in the TL are still evident, even when varying the properties in a relatively thin layer of sand. This behavior is likely to be caused by scattering at the interface between the ocean and the seabed, which transfers energy from compressional to shear waves in the region close to the interface. This demonstrates that it is important to have a reasonably accurate understanding of the acoustic properties of the upper layer of the seabed, even for relatively short ranges.

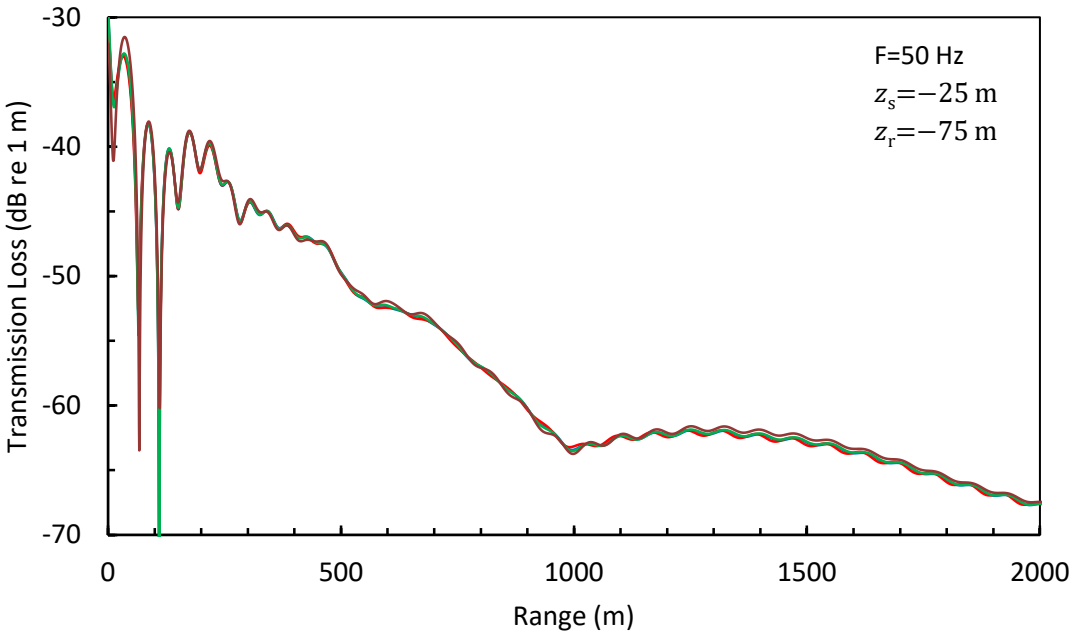

Figure 3 – TL for limestone seabed with damping: ; $\alpha_T = 0.1$ dB/λ; ; $\alpha_T = 0$ dB/λ; . $\alpha_T = 0.2$ dB/λ; ; $\alpha_T = 0.8$ dB/λ.

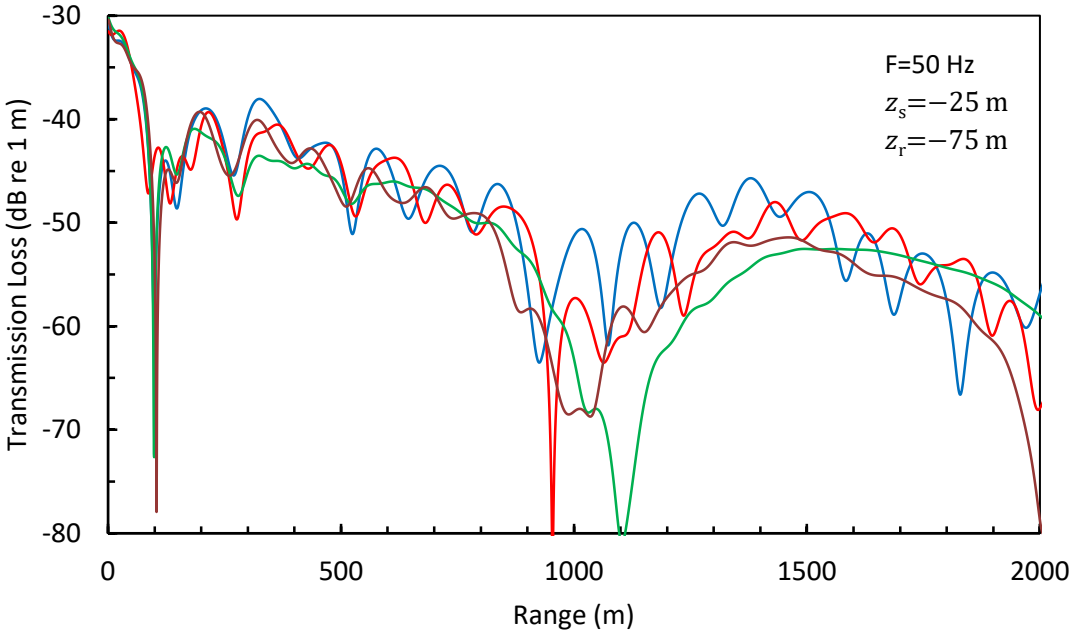

Figure 4 – TL for seabed with 10 m layer of sand with varying properties, above 300 m layer of limestone with fixed properties: ; $c_T = 400$ m/s; ; $c_T = 600$ m/s; $c_T = 200$ m/s; ; $c_T = 300$ m/s.

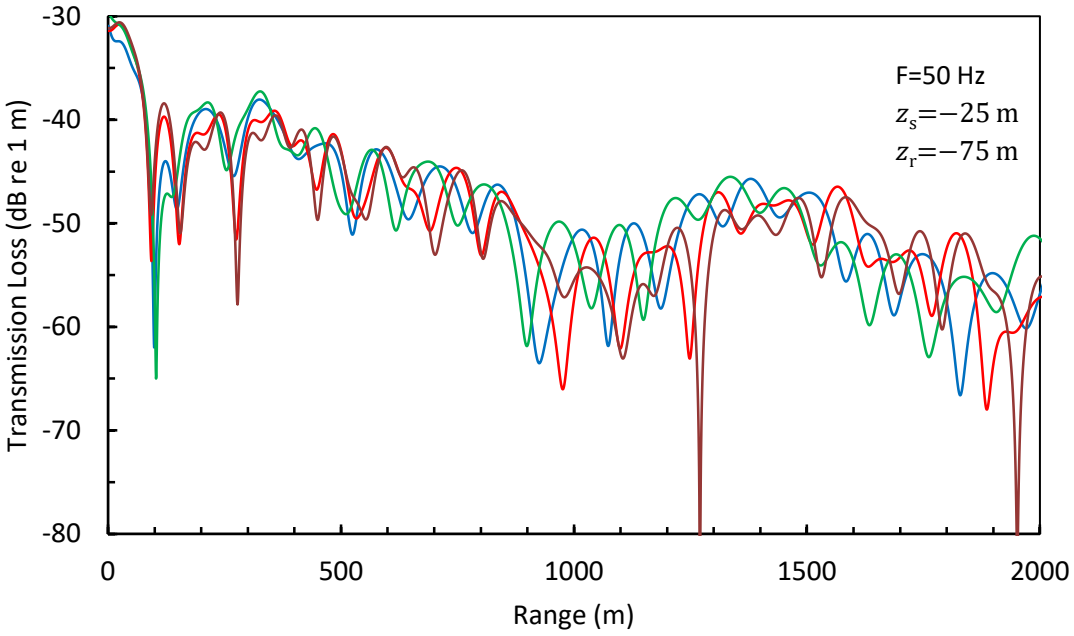

Figure 5 – TL for seabed with 10 m layer of sand with fixed properties, above 300 m layer of limestone with varying properties. ——; $c_T = 1315$ m/s; ——; $c_T = 1000$ m/s; ——; $c_T = 1600$ m/s; ——; $c_T = 1200$ m/s.

In Fig. 5 the properties of the sand are fixed and those of the limestone layer underneath the sand are changed (with both layers including damping). Figure 5 demonstrates that the properties of a second layer are still important when attempting to quantify sound propagation; however for this problem the influence is not as strong as that seen when varying the properties in the upper layer.

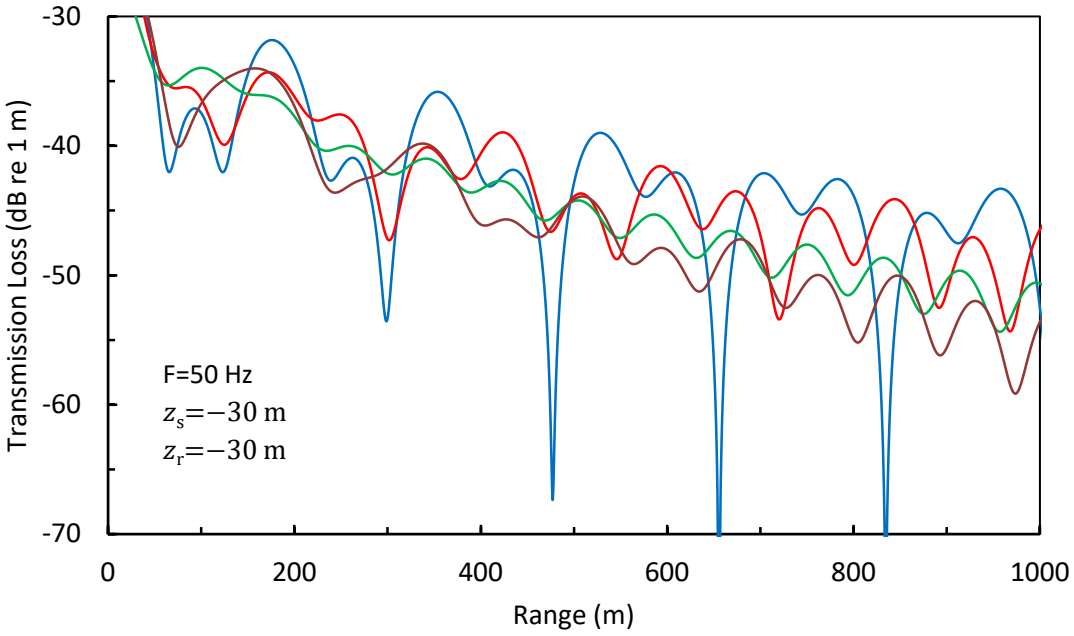

Figure 6 – TL for seabed with 10 m layer of sand with varying properties, above 300 m layer of limestone with fixed properties. ——; $c_T = 400$ m/s; ——; $c_T = 600$ m/s; ——; $c_T = 200$ m/s; ——; $c_T = 300$ m/s.

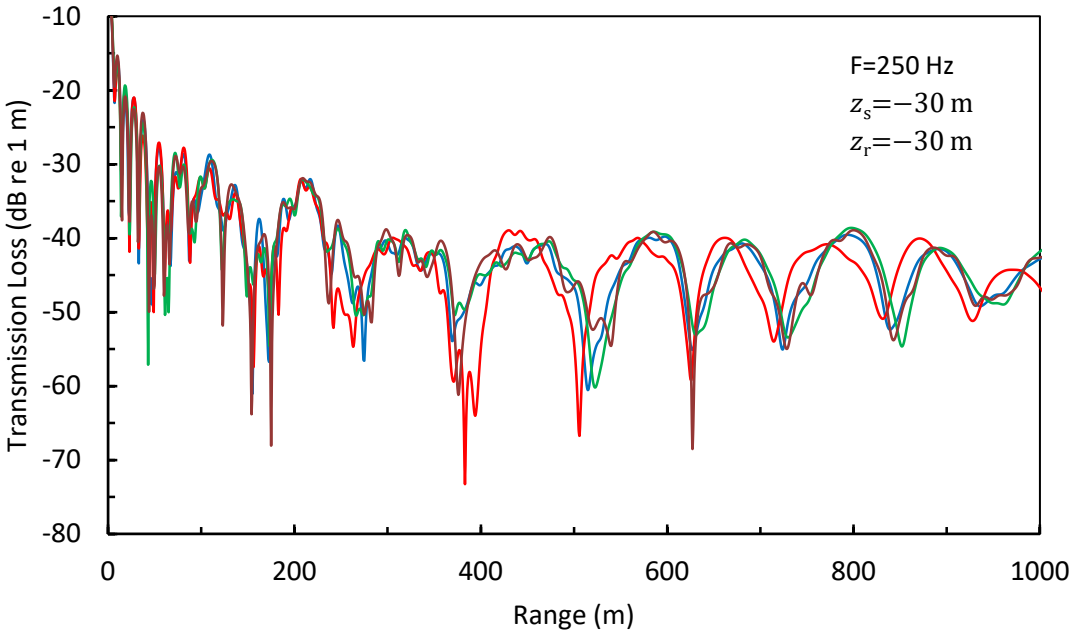

Figure 7 – TL for seabed with 10 m layer of sand with varying properties, above 300 m layer of limestone with fixed properties. ——— ; $c_T = 400$ m/s; ——; $c_T = 600$ m/s; ——— $c_T = 200$ m/s; ——; $c_T = 300$ m/s.

In Fig. 6 the depth of the ocean is reduced to 40 m and the sound source and receiver are both placed at a depth of 30 m. To accommodate a shallower ocean the range is reduced from 2 km to 1 km in Fig. 6. It can be seen in Fig. 6 that varying the properties of the upper layer of sand again leads to large differences in the TL. This difference continues to be significant and this further illustrates that achieving accurate predictions of TL in ocean acoustics is likely to be challenging because of the sensitivity of sound propagation to the shear properties of the seabed. However, if the frequency of excitation is increased to 250 Hz, then in Fig. 7 it is seen that the difference between predictions reduces. For a relatively short range, sound propagation now becomes less sensitive to the shear properties of the seabed. This is likely to be caused by the change in modal structure within the waveguide when the frequency is increased, so that those modes that are less sensitive to the shear properties are preferentially excited when compared to behavior at 50 Hz. This effect is likely to be problem dependent, however this further illustrates the complexity of the shallow waveguide problem.

4. CONCLUSIONS

This article uses a SAFE approach to compute the sound pressure distribution in an ocean waveguide. The SAFE method enables the sound propagation in the ocean to be coupled to viscoelastic wave propagation in the seabed, and through the use of PMLs it is shown to be possible to properly account for the limiting transverse boundary conditions. This makes the SAFE method well suited to modelling sound propagation in shallow oceans, and here it is shown that TL values can be very sensitive to the shear properties of the seabed. This present challenges for modeling sound propagation in shallow oceans, as measuring accurately the acoustic shear properties of viscoelastic materials over a wide frequency range can be difficult.

REFERENCES

1. Pekeris CL. Theory of propagation of explosive sound in shallow water. Geol. Soc. Am. Mem. 1948; 27.
2. Jensen FB, Kuperman WA, Porter MB, Schmidt H. Computational Ocean Acoustics. 2nd Ed., Springer, New York, 2011.
3. Etter PC. Underwater Acoustics Modeling and Simulation. 5th Ed., Taylor Francis, London 2018.
4. Etter PC. Recent advances in underwater acoustics and simulation. J. Sound Vib. 2001; 240: 351-383.

5. Westwood EK, Tindle CT, Chapman NR. A normal mode model for acousto-elastic ocean environments. J. Acoust Soc Am. 1996; 100: 3631-3645.
6. Porter M, Reiss EL. A numerical method for ocean-acoustic normal modes. J. Acoust Soc Am. 1984; 76: 244-252.
7. Porter M, Reiss EL. A numerical method for bottom interacting ocean-acoustic normal modes. J. Acoust Soc Am. 1985; 77: 1760-1767.
8. Duan W, Kirby R, Mudge P, Gan T-H. A one dimensional numerical approach for computing eigenmodes of elastic waves in buried pipelines. J Sound Vib. 2016; 384: 177-193.
9. Kalkowski MK, Muggleton MJ, Rustighi E. Axisymmetric semi-analytical finite elements for modelling waves unburied/submerged fluid-filled waveguides. Comput Struct. 2018; 196: 327-340.
10. Duan W, Kirby R. Guided wave propagation in buried and immersed fluid-filled pipes: Application of the semi analytic finite element method. Comput Struct. 2019; 212: 236-247.
11. Duan W, Kirby R, Mudge P. On the scattering of torsional waves from axisymmetric defects in buried pipelines. J. Acoust Soc Am. 2017; 141: 3250-3261.
12. Bergmann PG. The wave equation in a medium with a variable index of refraction. J. Acoust Soc Am. 1946; 17: 329-333.
13. Slaughter WS. The Linearized Theory of Elasticity, 1st Ed., Springer, Boston 2002.
14. Cummings A, Astley RJ. The effects of flanking transmission on sound attenuation in lined ducts. J Sound Vib. 1995; 179: 617-646.
15. Scandrett L, Frenzen CL. Bi-orthogonality relationships involving porous media, J. Acoust Soc Am. 1995; 98: 1199-1203.